Progress In Electromagnetics Research M, Vol. 92, 181–192, 2020

Estimation and Analysis of the Radio Refractivity, Its Gradient and the Geoclimatic Factor in Arctic Regions

Yamina Bettouche[1], Basile Agba[1], Ammar Kouki[1], Huthaifa Obeidat[2, *], Ali Alabdullah[3], Fathi Abdussalam[3], Sabir Ghauri[4], and Raed Abd-Alhameed[3]

Abstract—In this paper, local meteorological data of one year have been used to calculate the surface atmospheric radio refractivity (N) and estimate the vertical refractivity gradient (dN_1) as well as the geoclimatic factor (K) in the lowest atmospheric layer above the ground surface in the station Kuujjuaq (Quebec, Canada). In this region, the climate is arctic, characterized by very long and very cold winters (on average the temperature is below $-20°$C for almost 240 days per year). The precipitations are almost nonexistent, and the vegetation is scarce. Average daily, monthly, seasonal, and yearly variations of N, dN_1, and K are estimated and analysed. The obtained values of these indices are compared to the corresponding values provided by the ITU. The results show that the more negative values of dN_1 lie in the summer season. This is mainly due to the important variations of the temperature and humidity during this season. However, the estimated values lie in the limits mostly corresponding to standard refraction.

1. INTRODUCTION

Terrestrial fixed radio links operating at microwave frequencies on line-of-sight (LOS) are the widely used means for transmitting audio and video data from transmitter to receiver [1, 2]. The performance of the transmission depends not only on the precision of the user equipment but also on the state of the transmission medium (troposphere in this case). Troposphere is the region of the atmosphere extending from the surface of the earth up to a height of 8–10 km at polar altitudes, 10–12 km at moderate latitudes, and up to 18–19 km at the equator [3, 4]. The state of troposphere is determined by the climatic conditions: precipitation, temperature, pressure, water vapour pressure, etc. The variation of climatic conditions has an important impact on the quality of the propagation of radio waves [5, 6]. In the troposphere, the values of the main meteorological parameters (temperature, pressure, water vapour pressure) vary from one season to another and across different heights. Variation of these meteorological parameters leads to multipath propagation. The multipath propagation is an abnormal propagation mechanism which causes the attenuation or enhancement of the transmitted signal.

The presence of high refractive layers in the troposphere leads to a few fading mechanisms like beam spreading (defocusing), antenna decoupling, surface multipath, and atmospheric multipath. One of the more severe of these mechanisms is multipath fading [7, 8].

In the design of communication systems, it is necessary to take account of path delays and the percentage of time that a certain fade depth is not exceeded. The atmospheric refractivity N and vertical gradient dN_1 [9] are generally used for this evaluation. The value of the geoclimatic factor is an indicator of the fade depth. The ITU-R recommends estimating the geoclimatic factor based on

Received 7 February 2020, Accepted 16 April 2020, Scheduled 15 May 2020

* Corresponding author: Huthaifa Obeidat (h.obeidat@jpu.edu.jo).

[1] École de Technologie Supérieure, Lacime, Montréal, Canada. [2] Faculty of Engineering, Jerash University, Jordan. [3] Faculty of Engineering and Informatics, University of Bradford, Bradford, UK. [4] Department of Engineering and Mathematics, University of West England, Bristol, UK.

the local fading data measured in the region of interest. If these data are not available, ITU provides a procedure to find the value of the geoclimatic factor using the refractivity gradient in the region of interest [7].

Therefore, the performance of communication links is determined by the quality of the propagation of electromagnetic waves in the troposphere [10]. If the propagation quality is poor, two phenomena occur: decrease of the transmitted power level and distortion of the transmitted signal [11, 12].

To take into account the state of the atmosphere during the design of terrestrial communication links, the cumulative distribution of the refractivity gradient at a given height, h, is used as an assessment index [13]. The refractivity gradient can be determined based on two values of the radio refractivity. One of these values is determined at height, h, and the second at the surface ($h = 0\,\mathrm{m}$). There are two approaches to obtain the values of temperature, pressure, and water vapour pressure. One approach is to measure these parameters at different heights (radiosonde data). The second approach is to estimate the values of these parameters at a given height based on the measured values at some reference height. In this case, the second approach is used since the station Kuujjuaq, in Quebec, Canada yields only metrological data at the surface. Thereafter, these values are used to estimate the correspondent values at a given height using ITU recommended relationships.

The main contribution of this paper is to give recommendations for the design of the communication links based on the evaluation of the average daily, monthly, seasonal, and yearly distributions of radio refractivity, refractivity gradient in the first 65 meters above the ground.

The rest of this paper consists of the following sections. The second section describes the used methodology. The third section presents an analysis of the obtained results. The conclusion is given in the last section.

2. METHODOLOGY

In this study, the station Kuujjuaq is considered. This station is located in the North-East of Quebec at 58.1° latitude and −68.42° longitude, with an altitude of 39.9 m above sea level. The Canada environment provides local climatic parameters (temperature, dew temperature, humidity, pressure, etc.) stored in raw CSV format [14]. The data for the 2013 year are used in this paper. These files are converted into Excel files for further processing. An example of this file is shown in Table 1.

Table 1. A sample of the collected data for 2013.

Date	Time (hour)	Temperature, t (°C)	Dew Temperature, tr (°C)	Relative Humidity, H (%)	Pressure, P (kPa)
	00:00	11.5	9.1	85	100.74
	01:00	11.2	9.2	87	100.72
01-08-2013	...	...	...	...	...
	23:00	8.5	6.9	90	100.66
...	...	...	...	...	...
	00:00	3.2	0.3	81	100.12
	01:00	2.9	−0.6	78	100.11
31-08-2013	02:00	1.8	0	88	100.12
	...	...	...	...	...
	23:00	4.3	0.2	75	100.89

The flowchart of the used methodology to estimate the relevant parameters consists of several steps as shown in Fig. 1. The first step is to acquire the corresponding meteorological data measured at the surface. The second and third steps are to calculate, at the given height, the relevant parameters. The

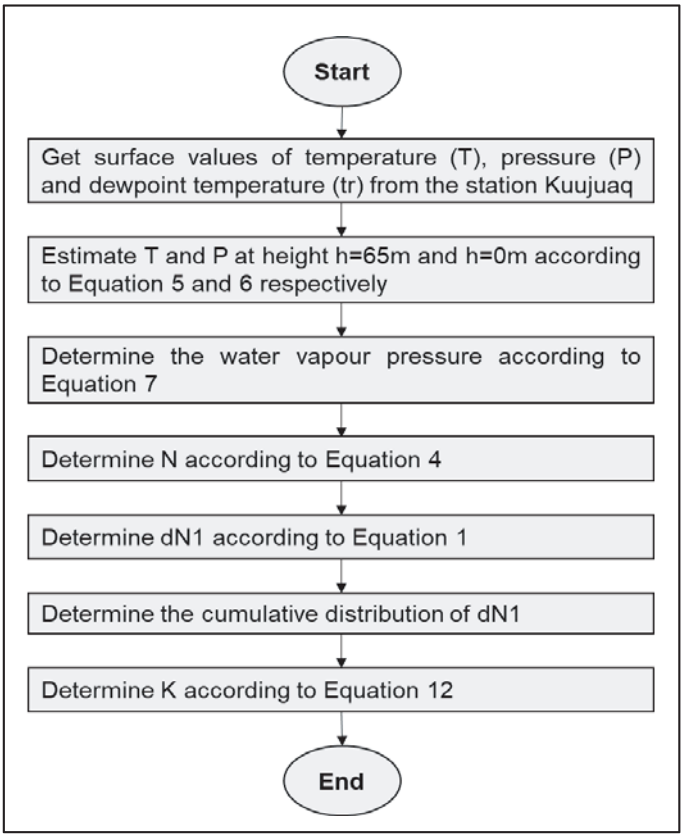

Figure 1. The flow chart of the used methodology.

fourth and fifth steps are to estimate the atmospheric radio refractivity (N) ant its gradient (dN_1), respectively. The occurrence probability of ducting and multipath conditions is estimated in the sixth step. Finally, the seventh step is to estimate the geoclimatic factor (K).

According to [10] dN_1 is determined by the following formulae:

$$dN_1 = (N_1 - N_s) / (h_1 - h_s) . \tag{1}$$

where N_1 is the atmospheric radio refractivity in N-units at height h_1 (65 m), and N_s is the surface atmospheric radio refractivity in N-units at height h_s ($h_s = 0$ km).

The variation of the atmospheric radio refractivity caused by the change of the meteorological parameters plays an important role in the study of the radio waves propagation in the troposphere. It is related to the refractive index, with n noted by the following relationship [12]:

$$N = (n - 1) 10^6 \tag{2}$$

The index n is determined by the following formulae:

$$n = \sqrt{\varepsilon \mu} \tag{3}$$

where ε is the relative permittivity, and μ is the relative permeability. In practice, N is often used instead of n because the variation of n relative to its mean value (1.0003) is very low (variations appear at the fifth and sixth decimals). The atmospheric radio refractivity at a given height, h, is estimated according to the formulae given in [12]:

$$N(h) = \frac{77.6}{T(h)} \left(P(h) + 4810 \frac{e(h)}{T(h)} \right) \tag{4}$$

where $T(h)$ is the absolute temperature (K); $P(h)$ is the total atmospheric pressure (hPa); and $e(h)$ is the water vapour pressure (hPa). There are two main ways to determine atmospheric radio refractivity, measuring by means of the refractometer or estimating from the meteorological data using Equation (4).

As seen from Equation (4) the atmospheric radio refractivity has two components. The first component is called dry component. This component varies with both pressure and temperature. The second component is called wet component. The latter component depends on the values of humidity and temperature. Depending on the season, these two components undergo various variations. In this paper, we will consider the following seasons: winter (December, January, and February), spring (March, April, and May), summer (June, July, and August), and autumn (October, September, and November). In summer, the wet component increases, and dry component decreases. This is because during this season the temperatures are high, and the humidity is low. However, in winter the tendencies are reversed.

In our case, the radiosonde data for the temperature $T(h)$, pressure $P(h)$, and water vapour pressure $e(h)$ are not available at the Kuujjuaq station. Only the surface data of these meteorological data are available. Therefore, to estimate the values of these parameters at given h, we use the formulas provided in [15]. The temperature $T(h)$ is given by:

$$T(h) = T_s - 6.5h \tag{5}$$

where T_s is the absolute temperature in Kelvin at the surface. The following formulae are used to determine the total atmospheric pressure $P(h)$ at given h [15]:

$$P(h) = P_s \left[T_s / (T_s - 6.5h)\right]^{-5.2558} \tag{6}$$

where P_s is the pressure in hPa at the surface. The water vapour pressure in hPa is determined by [15]:

$$e(h) = \frac{\rho(h) \times T(h)}{216.7} \tag{7}$$

where $\rho(h)$ is the water vapour density in g/m^3. It is determined as [15]:

$$\rho(h) = \rho_s e^{-\frac{h}{2}} \tag{8}$$

where ρ_s is the water vapour density at the surface. There are several methods to determine ρ_s. In this paper the following formulae are used [16]:

$$\rho_s = \frac{H_s \theta^6}{5.752} 10^{(10-9.834\theta)} \tag{9}$$

where $\theta = \frac{300}{T_s}$, H_s and T_s are the relative humidity and the absolute temperature in Kelvin at the surface, respectively. The relative humidity $H(h)$ in % at a given h is [12]:

$$H(h) = 100 \frac{e(h)}{e_s(h)} \tag{10}$$

where $e_s(h)$ is determined according to [17] by:

$$e_s(h) = 6.11 \times 10^{\frac{7.5t(h)}{237.7+t(h)}} \tag{11}$$

where $t(h)$ is the temperature $t(h)$ converted to degrees Celsius. In this paper, the geoclimatic factor, K, is determined based on the value of dN_1 [7]:

$$K = 10^{-4.6-0.0027dN_1} \tag{12}$$

3. RESULTS AND ANALYSIS

In this section, we will use the available hourly measured data at Kuujjuaq station and the methodology described in the previous section of this paper to estimate the relevant parameters and discuss the obtained results.

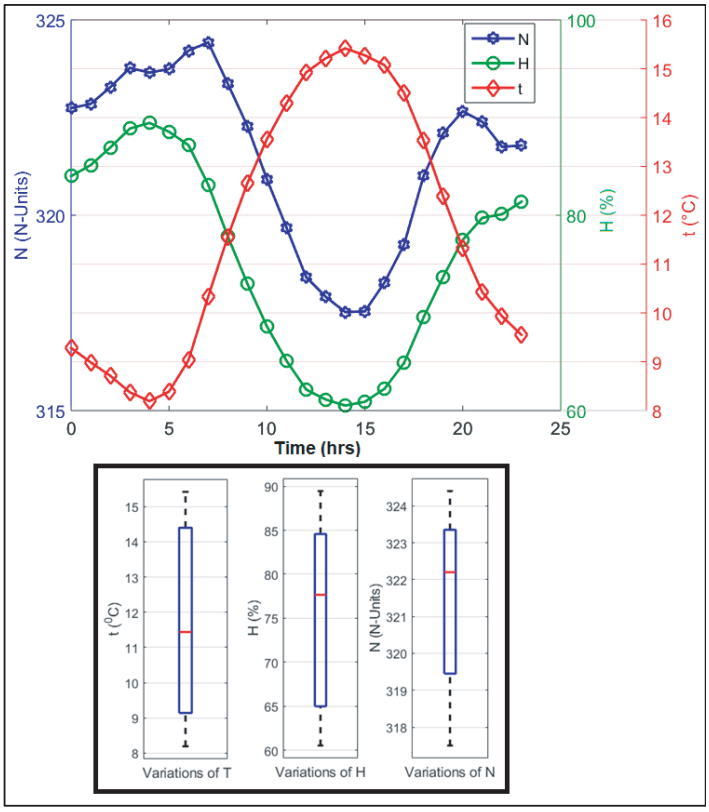

Figure 2. Average daily variations of N, H, and T at the surface on August 2013.

3.1. Analysis of the Surface Refractivity (N)

Figure 2 shows the average daily variations of N, H, and t in August 2013. It can be noted from the figure that T ranges from 8.19°C to 15.42°C. Its mean and median values are 11.70 and 11.44, respectively. H ranges from 60.52 to 89.45%. Its mean and median values are 75.48 and 77.66, respectively. N ranges from 317.5 to 342 N-Units. Its mean and median values are 321.47 and 322.2, respectively.

The analysis shows that the values of N are: very high, high, and low during the morning, night, and afternoon, respectively. Also, N has its highest value at 07 hours and the lowest value at 14 hours. Thus, in the early hours of the day, the occurrence of communication failure is more likely than in the rest of the hours. This is mainly because during the early hours of the day the humidity is high.

Figure 3 shows the mean yearly and seasonal probability density function (PDF) of the refractivity.

In order to identify the best-fit distribution for the seasonal PDF, the following procedure has been used. Firstly, the MATLAB function "*mle*" is used to determine the parameters of several distributions (Lognormal Distribution, Normal Distribution, Nakagami Distribution). Secondly, the Kullback-Leibler divergence is calculated using the MATLAB function "*ldiv*". The distribution with the smallest value of the Kullback-Leibler divergence has been selected. In our case, it is the Lognormal Distribution for monthly, seasonal, and yearly PDFs taken over the analyzed period. The obtained PDF shows that N is a log-normally distributed random variable with a mean value of $N_{mean\text{-}year\text{-}2013} = 314.17$ Units. The value of $N_{mean\text{-}year}$ is close to the ITU value ($N_{year\text{-}ITU} = 315.6$). Therefore, there is a good agreement of the obtained values and the ITU values.

Figure 4 shows the mean monthly variation of refractivity from December 2012 to November 2013. The highest value of N lies in August while the lowest value is found to be in November.

Figure 5 shows the mean seasonal variation of refractivity. The highest values of N lie in summer and winter. The values of N in spring and autumn are almost the same. Thus, in summer and winter, the occurrence of communication failure is more likely than spring and autumn seasons. This is also

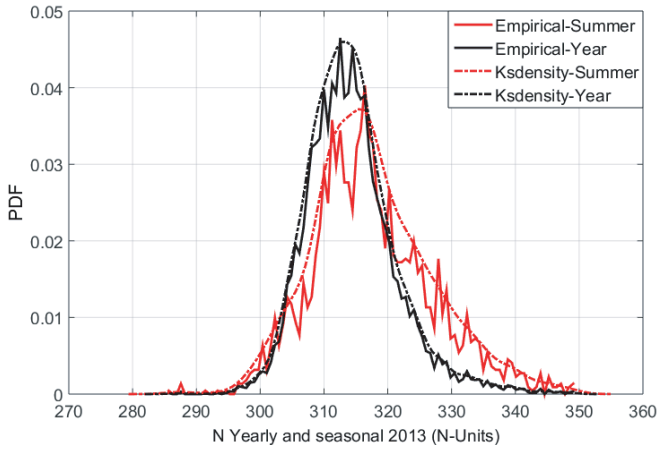

Figure 3. Seasonal PDF of surface refractivity.

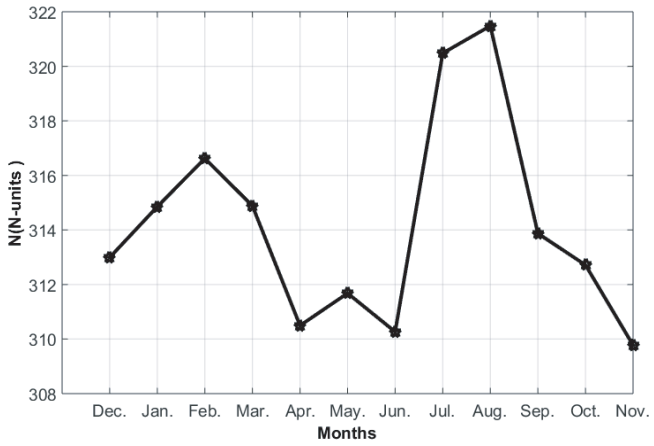

Figure 4. Mean monthly variation of refractivity.

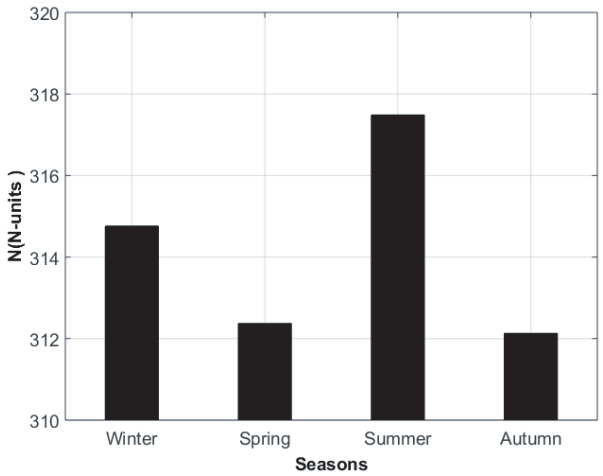

Figure 5. Mean seasonal variation of refractivity.

because in summer and winter the humidity is higher than in spring and autumn seasons.

The PDFs of the refractivity for several months are shown in Fig. 6. The monthly PDFs of the refractivity N_{month} obtained are also lognormally distributed random variables. For the Kuujjuaq station, it is observed that the yearly, monthly, and seasonal values of the refractivity follow a log-normal distribution, and also the high values of N tend to fall in summer, while the mean values of N in the months of July (320.5 Units) and August (321.5 Units) are the highest values.

3.2. Analysis of the Refractivity Gradient

An important index used in the design procedure for microwave links is the refractivity gradient, dN_1 [18, 19]. According to [19], there are four types of wave propagation:

a) Ducting: When $dN_1 < -157$ N-Units/km;
b) Super-refraction: When -157 N-Units/km $<= dN_1 <= -79$ N-Units/km;
c) Standard refraction: When -79 N-Units/km $< dN_1 <= 0$ N-Units/km;
d) Sub-refraction: When $dN_1 > 0$ N-Units/km;

Super-refraction and ducting can cause propagation well beyond the normal radio horizon, which has the potential to cause interference with nominally independent links. Sub-refraction causes fading

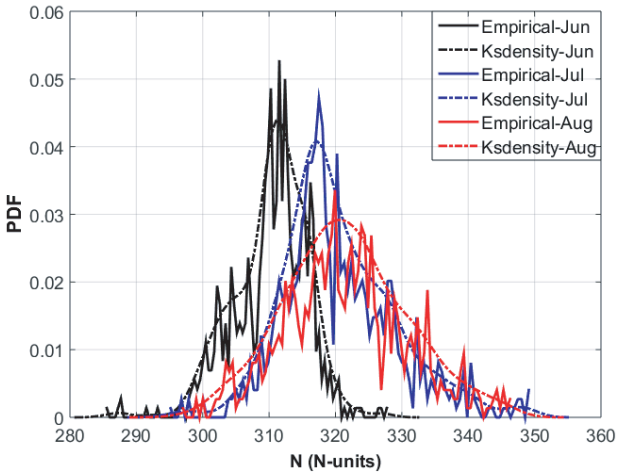

Figure 6. Monthly PDF of refractivity.

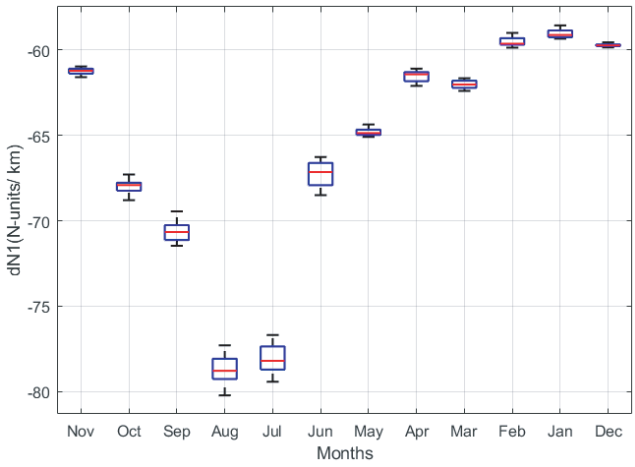

Figure 7. Average daily variations of dN_1.

on the intended link. Large negative values of dN_1 are also associated with an increased probability of deep, clear-air multipath fading [20].

3.2.1. Average Daily Variations of the Refractivity Gradient

The average daily variations of the resulting predicted refractivity gradient (dN_1) for various months (from December 2012 to November 2013) are shown in Fig. 7. From the variations shown in Fig. 7, it is clear that less and more negative values of the refractivity gradient lie in summer, autumn, spring, then winter. In the year 2013, the worst month is the month of August because more negative values of the average daily of dN_1 are found in this month. For each month, the average daily variations of dN_1 lie in the range where the standard refraction is the norm.

3.2.2. Monthly Variation of the Mean Refractivity Gradient

Figure 8 shows the average monthly variation of dN_1 (evaluated using Equation (1)), e, and T in 2013. The monthly variations of dN_1 are significant. The values oscillate between approximately -79 N-Units/km and -59 N-Units/km. The values are lower (i.e., more negative) during summer months than winter months. This can be attributed to the decreasing vapour content and pressure and the increasing temperature with height. From Fig. 8 one can also note that monthly mean values lie in the range -79 N-Units/km $< dN_1$-*mean* < -59 N-Units/km. Thus, standard refraction is the norm for this region. The cumulative distribution of the refractivity gradient determines the probability that a given value of the refractivity gradient is lower than a considered value.

Figure 9 shows the average monthly cumulative distributions of the refractivity gradient from December 2012 to November 2013.

It can be seen from Fig. 9 that all curves follow a similar trend. Almost for all percentages of time the more negative values of dN_1 lie in August. It can also be observed that for almost all percentages of time the less negative values of dN_1 lie in January. The more negative values of the refractivity gradient can be explained by the presence of the high temperature and high water vapour pressure, whereas the less negative values of the refractivity gradient can be explained by the presence of the low temperature and low water vapour pressure during the corresponding period of the year.

Figure 10 shows the average monthly variations of dN_1 for different time percentages of time. For 99% percent of time, minimum, maximum, and median values of dN_1 were: -65.68, -56.1, and -57.52 N-units/Km, respectively. For 90% percent of time, minimum, maximum, and median values of dN_1 were: -71.1, -57.4, and -58.8 N-units/Km, respectively. For 50% percent of time, minimum, maximum, and median values of dN_1 were: -78.53, -58.8, and -62.69 N-units/Km respectively. For 10% percentage of time, minimum, maximum, and median values of dN_1 were: -90.5, -60.7, and

−69.56 N-units/Km, respectively. For 1% percentage of the time, minimum, maximum, and median values of dN_1 were: −99.88, −62.11, and −76.64 N-units/Km, respectively. It was observed that in July and August during 10% of the time super-refraction condition would be observed. For the rest of the months and different percentages, the values of dN_1 lie between limits corresponding to standard refraction conditions.

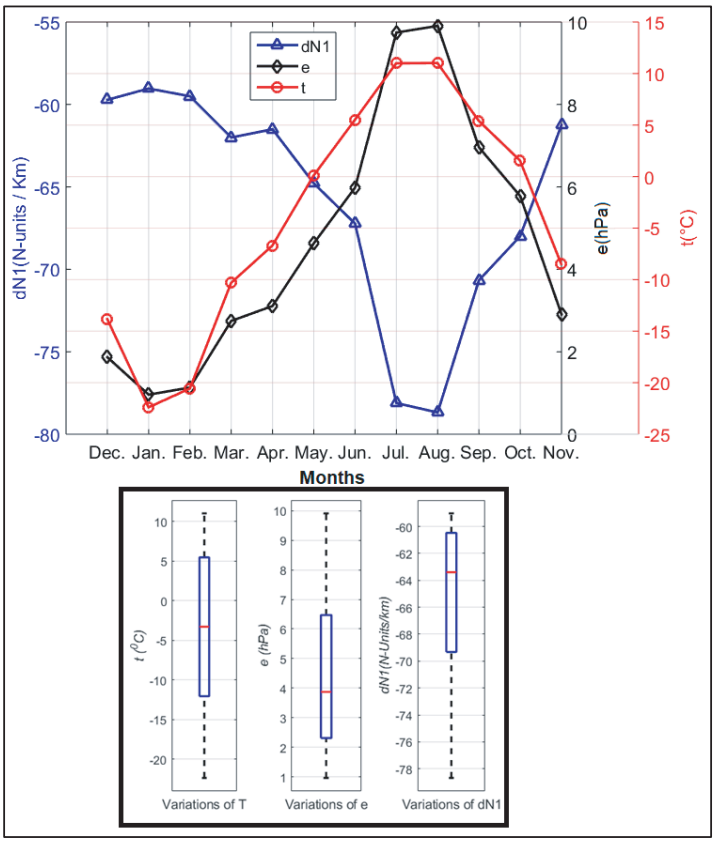

Figure 8. Mean monthly variations of dN_1 in 2013.

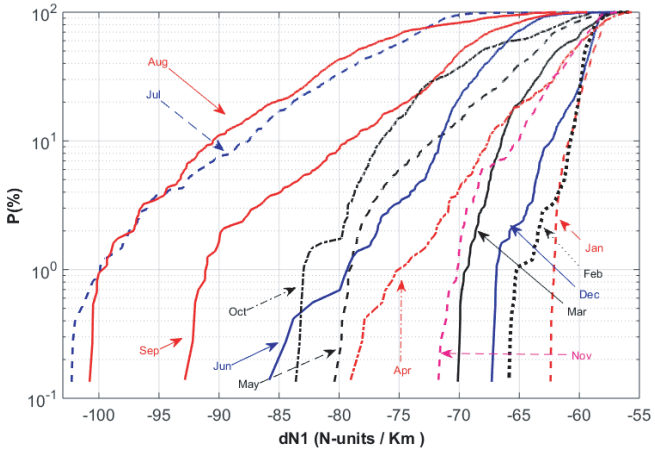

Figure 9. Average monthly cumulative distributions of dN_1 at 65 m.

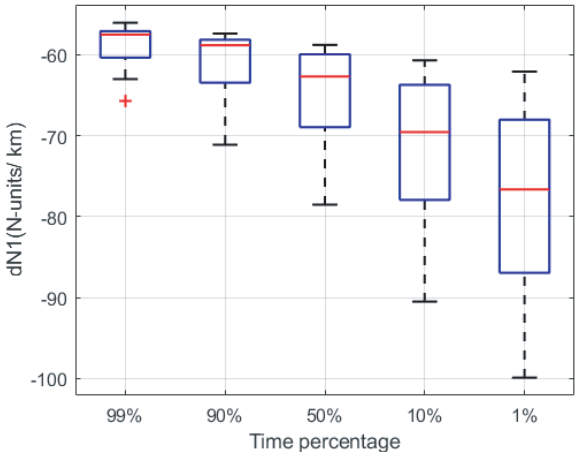

Figure 10. Average monthly variations of dN_1 for different percentages of time at 65 m in 2013.

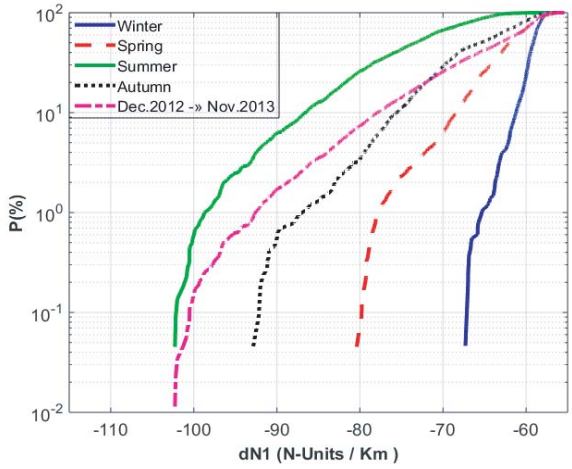

Figure 11. Average seasonal and yearly cumulative distributions of the dN_1 at 65 m in 2013.

3.2.3. Seasonal Variation of the Mean Refractivity Gradient

Average seasonal and yearly cumulative distributions of the refractivity gradient for December 2012 to November 2013 are shown in Fig. 11. The parameters derived from the yearly distributions are given in Table 2. The values of the refractivity gradient, which are not exceeded for a certain per cent of an average year, are compared with the values obtained according to the ITU-R model.

Table 2. Obtained values compared with ITU maps.

Percentage (%)	Obtained values (N-Units/km)	ITU values (N-Units/km)
1	-92.57	-250
10	-77.87	$-112,6$
50	-63.14	-41.8
90	-58.40	-23.8
99	-57.11	-3

For yearly results, we observe that for different percentages, the values of dN_1 are different from the corresponding values provided by ITU. For 1% and 10%, the value of the dN_1 obtained is higher than the correspondent ITU value. For 50%, 90%, 99%, the value of the dN_1 obtained is lower than the correspondent ITU value.

From Fig. 11 we note that for seasonal curves, more and more negative values of dN_1 occur from winter, spring, autumn to summer. From the yearly curve, we observe that the estimated yearly values of dN_1 for different percentages of time are different from the corresponding values provided by ITU. This difference is caused by the following factor. The ITU values have been determined using radiosonde data collected from 1955 to 1959 years. In this manuscript, the values are estimated based on data measured on surface in 2013 year. Due to climatic changes data used by ITU will be different from our data. Moreover, radiosonde data are more precise than the estimated data.

3.3. Analysis of the Geoclimatic Factor

Figure 12 shows the average daily variations of temperature (T), humidity (H) and the geoclimatic factor (K) observed at ground level in August 2013.

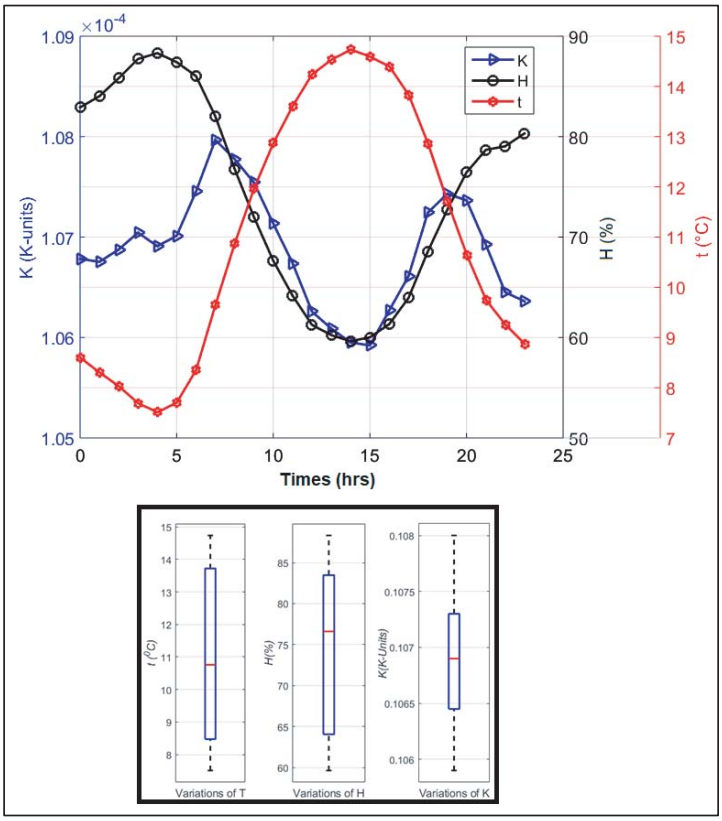

Figure 12. Average daily variations of T, H, and K at the surface on August 2013.

As seen in Fig. 12, T ranges from 7.5°C to 14.73°C. Its mean and median values are 11.02 and 10.76, respectively. H ranges from 59.63 to 88.31%. Its mean and median values are 74.46 and 76.60, respectively. K ranges from 0.106 to 0.1080 K-Units. It has the same value for the mean, and the median equals 0.1069. It is observed that for T there is a progressive increase of the values from 04 hours to 14 hours, and progressive decrease of these values during the remaining time of the day. For H, there is a progressive increase of the values from 00 hours to 04 hours and from 14 hours to 23 hours. From 04 hours to 14 hours there is a progressive decrease of these values. For K, it is observed that from 00 hours to 04 hours and from 19 hours to 21 hours, the values are almost constant. Also, there is a progressive increase of the values from 04 hours to 07 hours and from 15 hours to 19 hours. From 07 hours to 15 hours and from 21 hours to 23 hours there is a progressive decrease of the values.

Figure 13 shows the average daily variations of N, dN_1, and K. As seen from Fig. 13, N ranges from 312.5 to 319.2 N-units. Its mean and median values are 316.4 and 317.0, respectively. dN_1 ranges from −80.23 to −77.29 N-units/km. Its mean and median values are −78.68 and −78.79, respectively. K ranges from 1.0592e-04 to 1.0797e-04 K-Units. It has the same value for the mean, and the median equals 1.0687e-04. It is observed that from 04 hours to 07 hours and from 15 hours to 18 hours, there is a progressive increase of the values of K and progressive decrease of the values of dN_1. This is due to the high values of H. At 07 hours and 19 hours, there are more high values of the K and more negative values of dN_1. This is because in the same period of time there are high values of H. At 15 hours, there are more low values of K and high values of dN_1. This is because in the same period of time there are low values of H. Also from the figure, it can be observed that from 07 hours to 15 hours and from 20 hours to 23 hours, there is a progressive decrease of the values of K, and progressive increase of the values of dN_1. This is due to the progressive increase of the values of H. For K, it is observed that from 00 hours to 04 hours and From 18 hours to 20 hours, the values are almost constant.

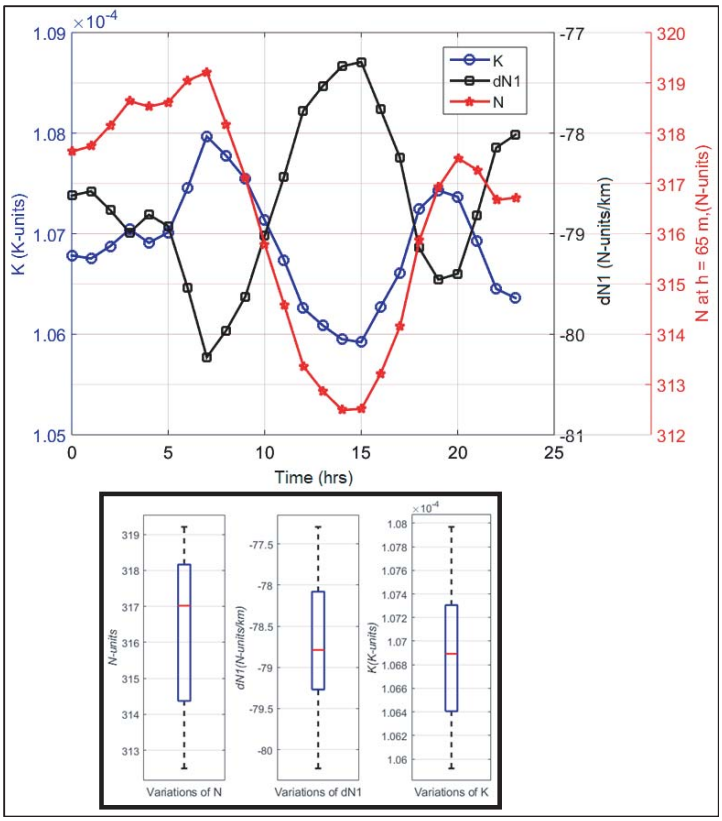

Figure 13. Average daily variations of N, dN_1, and K at $h = 65$ m on August 2013.

4. CONCLUSION

Previously, the assessments of the radio refractivity and refractive gradient have not been carried out in this region of Quebec. The results obtained in this paper show that the low values of the refractivity gradient lie from 06 hours to 09 hours and from 18 hours to 21 hours, and the maximum values lie from 12 hours to 16 hours. In these periods of day, there are high and low values of the humidity, respectively. The extreme values of the refractivity gradient appear mostly in summer. This is mainly because in summer the humidity and temperatures are much higher. The analysis of the estimated values shows that the standard refraction is the norm for the observed region. However, there is a low probability for the occurrence of super-refraction in July and August. In the future work, we plan to use the data for several years in order to see if there is some influence of the climatic changes on the values of the estimated parameters.

REFERENCES

1. Grabner, M., et al., "Multipath fading measurement and prediction on 10 GHz fixed terrestrial link," *15th Conference on Microwave Techniques COMITE 2010*, 145–148, IEEE, 2010.
2. Bogucki, J. and E. Wielowieyska, "Empirical season's fadings in radio communication at 6 GHz band," *Journal of Telecommunications and Information Technology*, 48–52, 2009.
3. Adediji, A., et al., "Radio refractivity measurement at 150 m altitude on TV tower in Akure, South West Nigeria," *Journal of Engineering and Applied Sciences*, Vol. 2, No. 8, 1308–1313, 2007.
4. Grabner, M., et al., "Parameters of vertical profiles of temperature humidity and refractive index of air in the lowest troposphere," *Proc. of 9th International Symposium on Tropospheric Profiling (ISTP)*, 2012.

5. Priestley, J. and R. Hill, "Measuring high-frequency humidity, temperature and radio refractive index in the surface layer," *Journal of Atmospheric and Oceanic Technology*, Vol. 2, No. 2, 233–251, 1985.
6. Kablak, N., "Refractive index and atmospheric correction to the distance to the Earth's artificial satellites," *Kinematics and Physics of Celestial Bodies*, Vol. 23, No. 2, 84–88, 2007.
7. Union, I. T., "Propagation data and prediction methods required for the design of terrestrial line-of-sight systems," *Recommendation of ITU-R*, 530-15, Geneva, 2015.
8. Norland, R., "Temporal variation of the refractive index in coastal waters," *2006 International Radar Symposium*, 1–4, IEEE, 2006.
9. Boumis, M., D. Rezacova, and Z. Sokol, "Calculation of vertical gradient of atmospheric refractivity making use of 3D objective analysis technique," *Electronics Letters*, Vol. 35, No. 18, 1583–1584, 1999.
10. Grabner, M. and V. Kvicera, "Clear-air propagation modeling using parabolic equation method," *Radioengineering-Prague*, Vol. 12, No. 4, 50–54, 2003.
11. Ali, S., et al., "Statistical estimation of tropospheric radio refractivity derived from 10 years meteorological data," *Journal of Atmospheric and Solar-Terrestrial Physics*, Vol. 77, 96–103, 2012.
12. ITU, "ITU-R P.453-11: The radio refractive index: Its formula and refractivity data," *ITU-R*, Geneva, 2015.
13. Brussaard, G., "Handbook on radiometeorology," *International Telecommunication Union*, Geneva, 1996.
14. Canada, G. O., "Données climatiques historiques," February 09, 2019, Available from: http://climat.meteo.gc.ca/.
15. ITU, "Reference standard atmospheres," *Recommendation of ITU-R*, 835-6, Geneva, 2017.
16. Liebe, H. J., "A contribution to modeling atmospheric millimeter-wave properties," *Frequenz*, Vol. 41, Nos. 1–2, 31–36, 1987.
17. Johnsnhweather, "Vapor pressure," October 09, 2019, Available from: http://www.johnsnhweather .com/formulas/vaporPressure.html.
18. Zilinskas, M., M. Tamosiunaite, M. Tamosiuniene, E. Valma, and S. Tamosiunas, "Gradient of radio refractivity in troposphere," *PIERS Proceedings*, 603–607, Moscow, Russia, August 19–23, 2012.
19. Turton, J., D. Bennetts, and S. Farmer, "An introduction to radio ducting," *Meteorological Magazine*, Vol. 117, 245–254, 1393, 1988.
20. AbouAlmal, A., et al., "Statistical analysis of refractivity gradient and β_0 parameter in the gulf region," *IEEE Transactions on Antennas and Propagation*, Vol. 61, No. 12, 6250–6254, 2013.